Bulgarian Journal of Meteorology and Hydrology

Национален институт по метеорология и хидрология

National Institute of Meteorology and Hydrology

Bul. J. Meteo & Hydro 24/2 (2020) 99-113

Future air temperature changes in the region of Sofia City during XXI century, modeled for two 30-year periods

Radoslav Evgeniev, Krastina Malcheva*

National Institute of Meteorology and Hydrology,
Tsarigradsko shose 66, 1784 Sofia, Bulgaria

Abstract: The present study aims to outline the possible air temperature changes and trends in the region of Sofia for two future periods, 2021-2050 and 2051-2080, based on data from meteorological observations and simulations of selected global circulation models with different horizontal resolutions for two climate change scenarios (RCP 4.5 and RCP 8.5). The results show an increase in monthly and seasonal air temperatures in the city area, both in the near future and in the longer time horizon compared to the reference period 1981-2010. The analysis of long-term variations of the simulated mean annual temperature reveals a significant positive trend in the period 1981-2080, which is better expressed under the scenario RCP 8.5 and comparable with the observed trend in the period 1981-2019.

Keywords: Air temperature, Sofia City, Climate projections, CMIP5, Climate change scenarios

1. INTRODUCTION

Worldwide increasing attention is being paid to the complex links between urbanization and climate change (e.g., WMO, 1996; Grimmond, 2007; Bazrkar et al., 2015). Today, over 55% of the world's population lives in urban areas, and this proportion is expected to increase to 68% by 2050 (United Nations, 2018). According to the assessment of the Organization for Economic Co-operation and Development (OECD), cities consume a great majority – between 60 to 80% – of energy production worldwide and account for a roughly equivalent share of global carbon dioxide emissions (OECD, 2010; 2013). The anthropogenized landscape in the large cities leads to forming a so-called urban climate and an urban heat island. It is a result of the interaction between the natural

* Krastina.Malcheva@meteo.bg

components, the elements of the urban environment (buildings, infrastructure), and the anthropogenic activity in the cities, where the natural landscape is gradually replaced by the complex structure of the growing urban areas (Niemelä et al., 2011).

The global warming phenomenon is related to the climate forcing by anthropogenic greenhouse gases (GHG) and aerosol emissions. Sutton et al. (2015) have investigated the link between change in global mean air temperature and regional air temperature changes around the world. It has been shown that global temperature explains 60%, or more, of the variance in local temperatures on decadal and longer timescales over a large fraction of the planet. In the context of internal variability of the climate system, this result implies that decadal changes in local temperatures over the instrumental records have been substantially shaped by a forced response. Although the direct contributions of urban warming to global climate are small, the increasing GHG emissions from urban areas are dominant anthropogenic sources. Urban warming, on the background of the predicted by climate change scenarios increase in summertime maximum temperatures and also in the frequency and magnitude of extreme conditions, suggests a greater risk of heatwaves in the future (Grimmond, 2007).

Sofia is the largest urban, administrative, and economic center of Bulgaria, where the anthropogenic impact on the local climate is well pronounced. In recent decades, the city has grown and covered more and more parts of the Sofia valley territory. According to the National Statistical Institute information (Dancheva et al., 2019), about 19% of the country‘s population is concentrated in the capital, which requires systematic regional surveys and climate analysis, especially in the context of contemporary climate change.

There is no uncomplicated answer about the degree of impact of the urban complex on the local climate system under the global warming process. The magnitude and nature of climatic changes are strongly influenced by local features, but as in other neighboring countries, and in Bulgaria, the multi-year course of the main climatic elements changed in recent decades, and these changes are well prominent in the large cities. Some peculiarities of the urban climate in Sofia were established even in the first decades of the last century (Ishirkov, 1903; Kirov & Krastanov, 1938). Later, the climate of the city has been studied by Hristov & Tanev (1970). In the monograph “Climate and Microclimate of Sofia” (Blaskova et al., 1983), the main characteristics of the heat island in the central city area have been explored and the first microclimatic zoning of Sofia and its surroundings have been proposed. Some recent studies (Vitanova & Kusaka, 2018; Dimitrova et al., 2019) investigated the characteristics of urban heat island and the impact of urbanization on the local climate using the Weather Research and Forecasting (WRF) model. The results confirmed the influence of urbanization (land use, building density and type) on the temperature distribution in Sofia City, as well as the significant increase of summer temperatures in the central urban zone compared to surrounding rural areas.

The present study aims to outline the possible air temperature changes and trends in the region of Sofia for two future periods, 2021-2050 and 2051-2080, based on data

from meteorological observations and simulations of selected global circulation models (GCMs), with different horizontal resolutions, under two climate change scenarios (RCP 4.5 and RCP 8.5).

2. STUDIED AREA, DATA AND METHODS

The city of Sofia is located in the central part of the Sofia Valley, with an average altitude of 550 m. The valley has an area of about 1200 km^2 (approximately 75 km long and about 20 km wide) and consists of two main parts – a valley bottom and fence mountain slopes. It stretches in a northwest-southeast direction between Balkan Mountains from the north and the mountains Viskyar, Lyulin, Vitosha, and Lozenska from the south. To the west, the valley borders with the low watershed between the rivers Slivnishka and Gaberska, and to the east, its border reaches the north-eastern branches of the Vakarelska Mountains.

Monthly average air temperature data from the Central Meteorological Station (CMS) of the National Institute of Meteorology and Hydrology (NIMH) Sofia in the period 1981-2019 are used as a reference dataset for evaluating the contemporary temperature regime in the city. Annual temperature anomaly, relative to the 1951-1980 baseline period, from Berkeley Earth's project BEST is used as a reference dataset for assessing long-term temperature variability. The project provides products of merged land-ocean data at 1°×1° grid back to 1850 (http://berkeleyearth.org/). BEST uses the spatially kriged version of HadSST3 (the global ocean temperature dataset of the UK Met Office) and homogenized land temperature observations data adjusted for station relocations, instrument changes, time of observation changes and other sources of inhomogeneity (Rohde & Hausfather, 2020).

Future air temperature changes in the region of Sofia are estimated by the simulated data from three GCMs: 1) CMCC-CM model of the Euro-Mediterranean Center on Climate Change (CMCC), 2) MPI-ESM-MR model of the Max Planck Institute for Meteorology (MPI-M), and 3) EC-Earth model of the European Centre for Medium-Range Weather Forecasts (ECMWF). These GCMs are included in the fifth phase of the Coupled Model Intercomparison Project (CMIP5), which brings together the world's major research centers developing GCMs and numerical modeling of the Earth's climate system, providing the framework for coordinated climate change experiments (Taylor et al., 2012). The results of simulations are freely available in the form of monthly fields (including the multi-model average, named as CMIP5 mean) through the Royal Netherlands Meteorological Institute's website – KNMI Climate Explorer (https://climexp.knmi.nl/start.cgi).

The above mentioned GCMs are supported by the European Network for Earth System modelling (ENES). The ENES community is strongly involved in the assessments of the Intergovernmental Panel on Climate Change (IPCC) and provides those predictions on which EU mitigation and adaptation policies are elaborated (https://portal.enes.org/

community/about-enes). Due to the small area of the studied region, the horizontal resolution of the models was a major factor in their choice.

The CMCC-CM model is a coupled atmosphere-ocean GCM with a horizontal resolution of 0.75°×0.75°. The atmospheric model component is ECHAM5 (Roeckner et al., 2003), and the ocean component is the global ocean model OPA 8.2 (Madec et al., 1998). The ocean model also provides sea ice cover and thickness to the atmospheric model. The relatively high coupling frequency adopted allows an improved representation of the interaction processes occurring at the air-sea interface (Scoccimarro et al., 2011).

The EC-Earth model has evolved from the seasonal prediction system of ECMWF (Hazeleger et al., 2010). The CMIP5 version of EC-Earth (with a horizontal resolution of 1.125°×1.125°) is based on the ECMWF integrated forecasting system (IFS) and the NEMO version 2 ocean model (OPA9 with the LIM2 sea ice model). Compared to other related models with similar complexity, the model performs well in simulating tropospheric fields and dynamic variables (Hazeleger et al., 2012).

The MPI-ESM family is a comprehensive Earth-System Model (ESM), consisting of component models for the ocean and sea ice (MPIOM), the atmosphere (ECHAM6), and the land surface (JSBACH). These components are coupled through the exchange of energy, momentum, water and important trace gases such as carbon dioxide (Marsland et al., 2003). The MPI-ESM-MR model has a horizontal resolution of 1.875°×1.875° and overall reasonably reproduce the temperature signal of the 20th century in comparison to HadCRU4.1 data. The model shows a tendency to reduce the ocean heat uptake efficiency toward a warmer climate, and hence acceleration in warming in the later years (Giorgetta et al., 2013).

Projections of the future climate provided by GCMs simulations serve as a basic and irreplaceable data source for a large spectrum of climate change studies. The future changes in average annual and seasonal air temperatures in the region of Sofia during the periods 2021-2050 and 2051-2080 are estimated by the simulated data from the selected GCMs under two climate change scenarios, RCP 4.5 and RCP 8.5, included in the Fifth Assessment Report (AR5) of the IPCC. The report introduced four scenarios depending on the so-called representative concentration pathways (RCPs): RCP 2.6, RCP 4.5, RCP 6, and RCP 8.5 (the numerical value after the abbreviation denotes the possible range of radiative forcing in W/m^2 at the end of the century) – see for details: IPCC, 2014.

The RCP 4.5 scenario envisages stabilization of concentrations through the application of measures to limit GHG emissions. According to this scenario, GHG emissions will increase until 2040, after which they will start to decrease, and by 2100 the radiative forcing is expected to be 4.5 W/m^2, which corresponds to an approximate concentration of 650 ppm CO_2 equivalent.

The RCP 8.5 scenario is strictly pessimistic and assumes a rapid increase in population, poor technological development (without implementing measures to reduce GHG emissions), increasing poverty, and, on the other hand, high energy consumption

and increasing emissions (Van Vuuren et al., 2011). The radiative forcing will increase to 8.5 W/m^2 by 2100, which corresponds to concentrations of 1370 ppm in CO_2 equivalent.

Because of their coarse spatial resolution, GCMs cannot reproduce the climate processes at a regional and local level. There are two main approaches to improve the models' output spatial/temporal resolution: statistical and dynamical downscaling. Dynamical downscaling uses a higher resolution regional climate model (RCM) whose boundary conditions and physical principles to reproduce local climate are supplied by a GCM. Since the RCM is nested in a GCM, the overall quality of dynamically downscaled RCM output is tied to the accuracy of the large-scale forcing of the GCM and its biases (Seaby et al., 2013). Statistical downscaling uses relatively simple empirical relationships between the observed climate and the GCM output for the same historical period. This approach can produce site-specific climate projections, but it relies on the critical assumption that the relationship between present large-scale circulation and local climate remains valid under different forcing conditions of possible future climates (Zorita & von Storch, 1999; Diaz-Nieto & Wilby, 2005).

Perhaps the most straightforward downscaling method for rapid climate change impact assessment is the Delta Method, which consists of calculating "change factors" (CFs) of the reference climatology (given for the site or region of interest) against the equivalent variables for the GCM grid-box closest to the target site. This method preserves the spatial and temporal characteristics of historical data but also supposes that the spatial pattern of the present climate remains unchanged in the future (Wilby et al., 2004; Diaz-Nieto & Wilby, 2005). Since the method assumes normally distributed data, its applicability is limited mostly to monthly or long-term averages. Typically, CFs are calculated as anomalies between the GCM future projections under a given scenario and GCM simulations for some historical period. After that, these CFs are applied to the historical period observed data to generate time series for the future climate. For unbounded meteorological variables, such as temperature, the formula could be written as follow:

$$X(t) = X_{raw}(t) - \left(\overline{X}_{ref} - \overline{O}_{ref}\right) \; O_{fu}(t) = O_{ref}(t) + \left(\overline{X}_{fu} - \overline{X}_{ref}\right) \quad (1)$$

where $X(t)$ is the adjusted time series; the indices refer to the reference period (*ref*) and future period (*fu*); CF is shown in parentheses. Observations are marked with *O* and the average values – with an overline.

In the present study, the average monthly, seasonal, and annual air temperature values for the two future periods are calculated from the adjusted monthly temperature data (Eq. 1). The usual partitioning of months by seasons has been used (winter – December, January, February; spring – March, April, May; summer – June, July, August; and autumn – September, October, November).

The freely available R Software Version 3.6.2 (R Core Team, 2019) and in particular, the R-package 'trend' (Thorsten, 2020), has been used to evaluate the significance and magnitude of air temperature trends in the studied periods. The non-parametric

Mann-Kendall test (Kendall, 1975) is commonly applied to detect monotonic trends in climatic and hydrological data. The null hypothesis is that the data come from a population with independent realizations and are identically distributed. The statistical significance of the trend was assessed at the standard significance level of 0.05. Sen's method (Sen, 1968) is used to estimate the slope of the trend for a linear rate of change. All computations have been made using the scripting language R under the integrated development environment RStudio Version 1.2.5033 (RStudio Team, 2019).

3. RESULTS

Monthly mean air temperature data from the model CMCC-CM, generated by the KNMI Climate Explorer web application (https://climexp.knmi.nl/start.cgi), have been averaged for territory with coordinates: lon = 22.875 ÷23.625E and lat = 42.661 ÷ 43.409N, which is closest to the study area and for this reason shows the highest correlation with the reference station data. About the model with the lowest resolution (MPI-ESM-MR), the averaging zone has coordinates: lon = 21.563 ÷ 23.438N, lat = 41.036 ÷ 42.901N. Figure 1 shows the monthly temperature profiles by the raw output data from the selected models in the reference period 1981-2010.

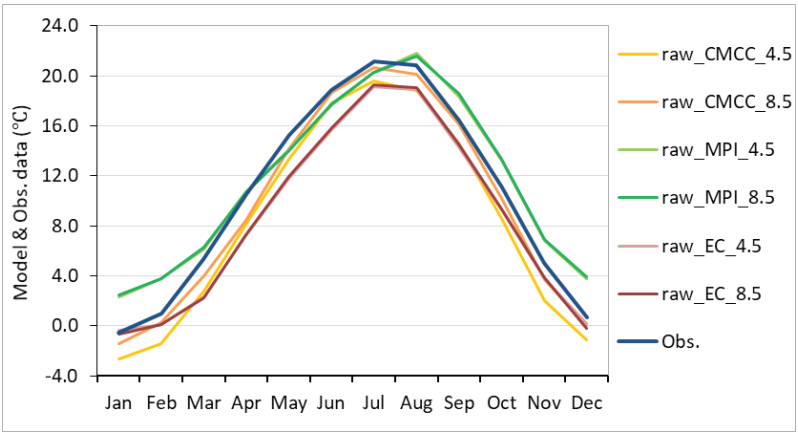

Fig. 1. Monthly temperature profiles derived from observation data (dark blue line) and raw output data from the selected models in the reference period 1981-2010

The calculated CFs for 2021-2050 and 2051-2080 under RCP 4.5 and RCP 8.5 scenarios vary from about 0 to 5°C. The projected mean annual temperature in the city area (averaged by the three models for each scenario) is 11.5/11.8 °C in 2021-2050 and 12.4/13.4 °C in 2051-2080 for RCP 4.5/RCP 8.5, respectively. The average increase of monthly mean temperatures in 2021-2050 is +1.0°C for RCP 4.5 and +1.3°C for RCP 8.5. The maximum rise of temperatures (+2.1-2.4°C) is predicted by CMCC-CM (RCP

8.5) for the cold half-year. The other GCMs predict an increase in temperature with 2.0°C and more only in July or August (Fig. 2).

In general, the model CMCC-CM forecasted the largest increase in monthly mean temperatures in the period 2051-2080 compared to the reference period for both climate change scenarios. The differences vary from +1.7°C in May to +3.6°C in August for RCP 4.5 and from +2.8°C in May to +5.0°C in January for RCP 8.5. Only in June and July, the MPI-ESM-MR shows a larger temperature raising by about 0.4°C under the RCP 8.5 scenario (up to +3.7°C and +4.6°C, respectively) – Fig. 3.

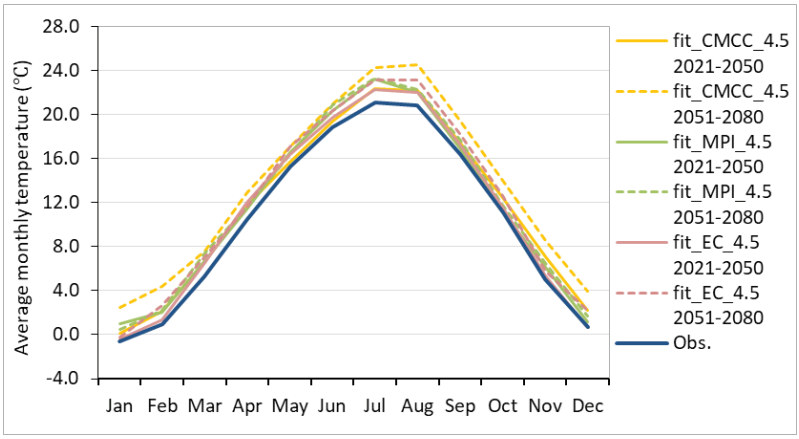

Fig. 2. Monthly temperature profiles for the periods 2021-2050 and 2051-2080 under scenario RCP 4.5 compared to the observations (dark blue line) in the reference period 1981-2010

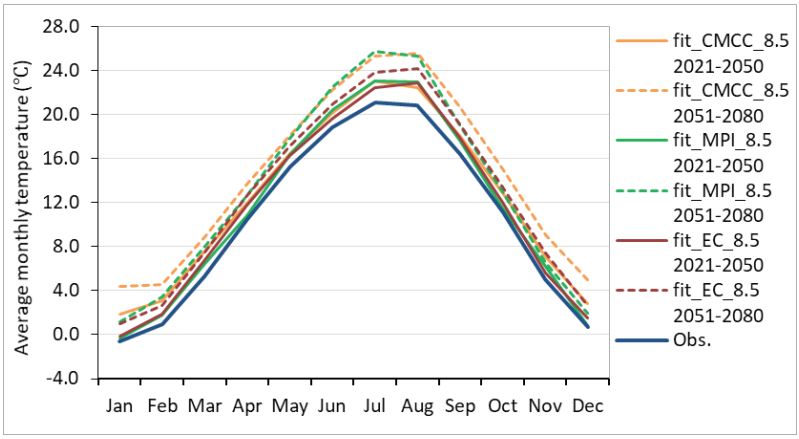

Fig. 3. Same as Fig. 2. but for scenario RCP 8.5

Table 1 presents the calculated trend coefficients of projected mean annual and seasonal air temperatures in Sofia in the period 2021-2050. For RCP 4.5 scenario, only

the model EC-Earth predicts a negative trend for the annual and seasonal temperatures (except for autumn), which is not statistically significant. A positive, statistically significant trend is expected only in summer (0.74°C/decade) and annually (0.52°C/decade) according to the CMCC-CM simulations. For RCP 8.5 scenario, two of the models predict statistically significant positive trends: MPI-ESM-MR – in winter (0.57°C/decade), summer (0.33°C/decade), and annually (0.40°C/decade); and CMCC-CM – in spring (0.39°C/decade) and annually (0.37°C/decade).

Table 1. Trend coefficients of annual and seasonal air temperatures (°C/decade) in Sofia in the period 2021-2050 for the selected GCMs and scenarios

Scenario	GCM	Winter	Spring	Summer	Autumn	Yearly
RCP 4.5	MPI-ESM-MR	0.37	0.04	0.14	0.33	0.26
	CMCC-CM	0.54	0.45	**0.74***	0.34	**0.52***
	EC-Earth	-0.09	-0.04	-0.52	0.33	-0.05
RCP 8.5	MPI-ESM-MR	**0.57***	-0.03	**0.33***	0.34	**0.40***
	CMCC-CM	0.12	**0.39***	0.47	0.58	**0.37***
	EC-Earth	0.77	0.13	0.36	0.22	0.30

**Statistically significant trend*

Table 2 shows trend coefficients of mean annual and seasonal air temperatures in the period 2051-2080. Only MPI-ESM-MR (RCP 4.5) predicted negative but statistically insignificant trends. In winter, there are not expected statistically significant trends for both scenarios.

Table 2. Same as Table 1 but for the period 2051-2080

Scenario	GCM	Winter	Spring	Summer	Autumn	Yearly
RCP 4.5	MPI-ESM-MR	0.32	-0.38	-0.03	-0.37	-0.09
	CMCC-CM	0.67	**0.98***	**0.95***	**0.81***	**0.81***
	EC-Earth	0.49	**0.48***	0.47	0.10	**0.50***
RCP 8.5	MPI-ESM-MR	0.02	**0.53***	**1.46***	**0.70***	**0.65***
	CMCC-CM	0.42	0.55	**0.86***	**0.88***	**0.87***
	EC-Earth	0.52	**0.58***	**1.19***	0.55	**0.79***

**Statistically significant trend*

Concerning mean annual air temperatures, the trend is not statistically significant only for MPI-ESM-MR (RCP 4.5). For the other cases, the values vary from 0.50°C/decade for EC-Earth (RCP 4.5) to 0.87°C/decade for CMCC-CM (RCP 8.5). The highest statistically significant trend coefficients by seasons are as follows: 0.98°C/decade in spring for CMCC-CM (RCP 4.5), 1.46°C/decade in summer for MPI-ESM-MR (RCP 8.5), and 0.88°C/decade in autumn for CMCC-CM (RCP 8.5).

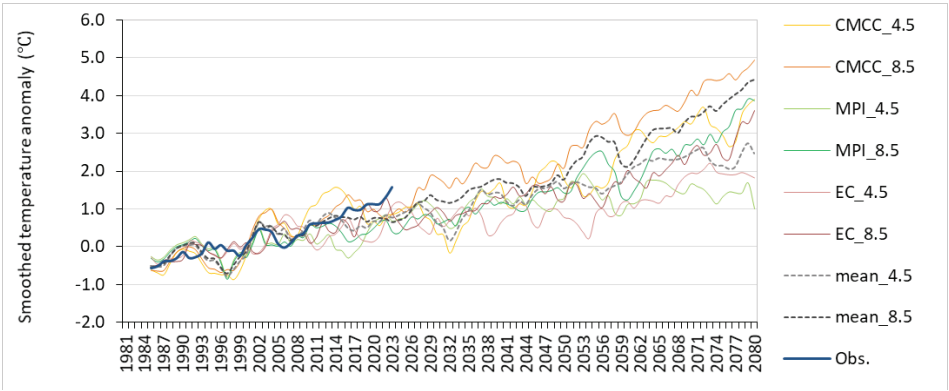

Fig. 4. Long-term variations of smoothed annual temperature anomaly (relative to 1981-2010) based on the observations in the period 1981-2019 (dark blue line) and GCMs simulations (1981-2018); mean_4.5 and mean_8.5 represent a simple averaging over the models for the respective scenario. The smoothed values have been obtained by a 5-year moving average.

The analysis of long-term variations of projected mean annual temperatures (presented in Figure 4 by smoothed anomalies) shows a significant positive trend in the period 1981-2080, which is better expressed for RCP 8.5 (about 0.46°C/decade, averaged over the models). This trend is comparable with the observed trend in the period 1981-2019. Is RCP 8.5 the more likely climate change scenario for Sofia City in the coming decades?

Friedlingstein et al. (2014) show that CO_2 emissions "track the high end" of emissions scenarios due to lower than anticipated carbon intensity improvements of emerging economies and higher global gross domestic product growth. In the absence of more stringent mitigation, these trends are set to continue. Many studies established that growing global mean temperature does not depend on the emissions pathway but rather is proportional to cumulative CO_2 emissions since the pre-industrial era. The relationship between global annual temperature increases and cumulative global CO_2 emissions can be quantified by the transient climate response to cumulative carbon emissions with values ranging from about 0.7 to 2.5°C per 1000 GtC, depending on the used model (IPCC, 2014). The growth rate in atmospheric CO_2 level increased from 1.7±0.07 GtC yr^{-1} in the 1960s to 4.7±0.02 GtC yr^{-1} during 2008-2017 with important decadal variations. Cumulative emissions through to the year 2018 increase to 625±80 GtC (Le Quéré et al., 2018).

For assessing potential impacts of the urbanization process on the local temperatures in Sofia against the background of global/regional warming, the annual air temperature anomaly from the project BEST, obtained through an interactive application of Carbon Brief website (https://www.carbonbrief.org), is used as a reference dataset. The application combined observed temperature changes with future climate model projections for every different part of the world in a 1°×1° grid. For any grid cell,

the BEST's historical temperature data 1850-2017, both by year and with a 10-year smoothed average, and the projected warming under the four RCP scenarios from 1999 through to 2100 can be downloaded in CSV file format.

Since the mid-1970s, observation data show faster warming (relative to the reference data tendency), which is in line with the increasing urbanization pace in this part of the city where the meteorological station is located (Figure 5). In the last 35 years, the mean urbanization-related warming is 0.34°C. The extra warming trend is estimated as 0.06°C/decade in 1953-1975, 0.25°C/decade in 1976-1990, and about 0°C/decade in 1991-2017. Urbanization-related (urban) warming, considered here as the difference in annual temperature anomalies of observations and reference data, concerns climate signal recognition rather than an urban heat island evaluation; accordingly, the trend in this climate signal can be defined as an extra warming trend.

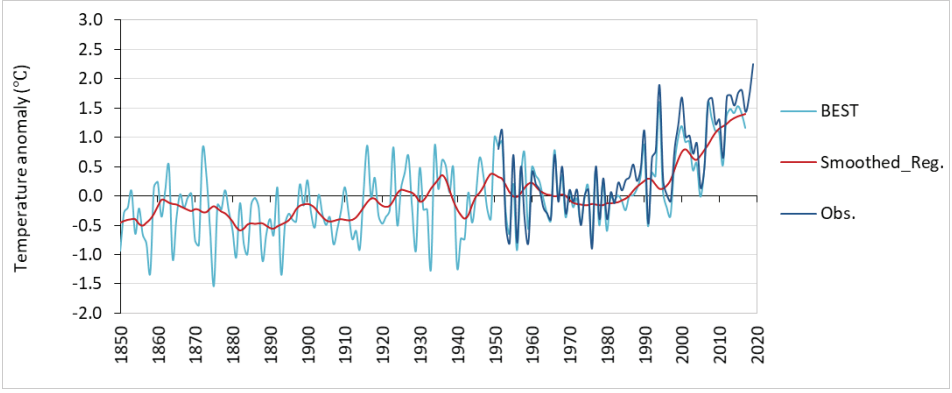

Fig. 5. Long-term variations of annual temperature anomaly (relative to 1951-1980) in the region of Sofia based on observations in the period 1953-2019 (dark blue line) and BEST's data (1850-2017), provided by Carbon Brief (https://www.carbonbrief.org). The smoothed average is obtained using a local regression approach with a 10-year period for calculation.

The determination of periods in the local urbanization development is based on: 1) freely available historical information about the construction of the residential complexes and adjacent infrastructure and 2) analysis of annual temperature anomaly calculated from the observations for the baseline period of reference data. As seen in Figure 6, both urban warming and the extra warming trend (calculated by a 10-year running window) reached a maximum in the late 1980s (0.63°C in 1987 and 0.051°C/year for 1978-1987) when the anthropogenized landscape is almost completely formed. Despite the increasing building density in recent decades, the climate signal of urbanization-related warming weakens. The results are consistent with the findings of Shen et al. (2020). The authors investigate the long-term effect of rapid urbanization in Shanghai in 1961-2017 and define three successive stages in the urban heat island evolution: initial slow growth stage, rapid growth stage, and obvious deceleration stage.

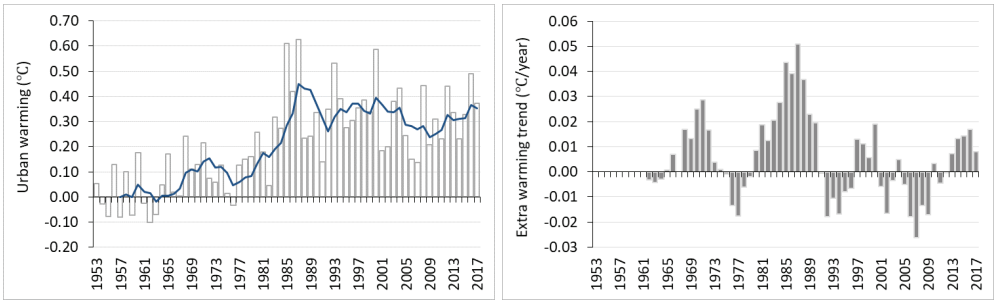

Fig. 6. Long-term variations of urban warming (left) and extra warming trends, calculated by 10-year running window (right). The smoothed values of urban warming (dark blue line) have been obtained by a 5-year moving average.

Carbon Brief provides temperature projections for each RCP scenario as a multi-model mean of temperature fields from 38 CMIP5 GCMs downscaled to 1°×1° resolution, then converted into adjusted anomalies to be comparable to BEST's dataset over the period 1999-2017 (Figure 7). Multi-model mean (obtained by simply averaging over the ensemble of models) is the most common and widely used approach. There is some evidence that the "mean model" result provides an overall best comparison to observations for climatological mean fields (Wang et al., 2018). In the period 1999-2080, the projected regional mean annual temperature increases with 0.52°C/decade for RCP 8.5 and almost half for RCP 4.5 (0.28°C/decade) with an expectation to reach 13.5°C in 2080 under the worse scenario. The BEST's data and observations show similar trends in 1999-2017: 0.38°C/decade and 0.39°C/decade, respectively.

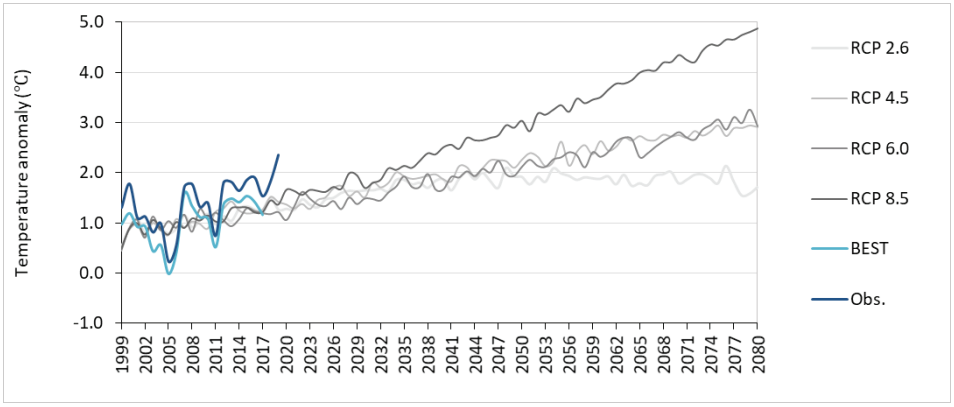

Fig. 7. Long-term variations of annual temperature anomaly (relative to 1951-1980) in the region of Sofia based on observations in the period 1999-2019 (dark blue line), BEST's data (1999-2017), and adjusted CMIP5 multi-model mean under various RCP scenarios (1999-2080), provided by Carbon Brief (https://www.carbonbrief.org).

Oleson (2012) analyzed the temperature in cities simulated by the CMIP5's model CCSM4 under different RCP scenarios to examine how much differently urban and rural areas might respond to climate changes. Globally averaged, urban and rural air temperature both increase in the future, according to the degree of radiative forcing. Climate change increases the number of warm nights in urban areas substantially more than in rural areas. However, the expected urban heat island intensity at the end of the twenty-first century is similar to present-day (1986–2005) in RCP4.5 and RCP2.6 and slightly decreases in RCP8.5, due to the changes mainly in evaporation and diurnal temperature range in rural areas under the global warming process.

As a whole, the short analysis presented here, confirm that urbanization-related warming does not determine the long-term changes in the mean annual air temperature in the city. The weak urbanization effect on the local climate system is expected to decrease in the coming decades against the background of increasing climate change under the global/regional warming process in the worst climate change scenario.

4. CONCLUSIONS

Based on the data from meteorological observations and simulations by three GCMs (with different horizontal resolutions), the possible tendencies of the air temperature change in the region of Sofia in the periods 2021-2050 and 2051-2080 have been analyzed under two climate change scenarios (RCP 4.5 and RCP 8.5).

The average increase in monthly temperatures during the period 2021-2050, compared to the reference period 1981-2010, is +1.0°C for the RCP 4.5 scenario and +1.3°C for the RCP 8.5 scenario, with a maximum of +2.2-2.4°C in the cold half-year, according to the CMCC-CM (RCP 8.5). In general, the CMCC-CM model predicts the largest increase of average monthly air temperatures in the period 2051-2080 – the changes vary from +1.7°C in May to +3.6°C in August for RCP 4.5 scenario and from +2.8°C in May to +5.0°C in January for RCP 8.5 scenario.

In the period 2021-2050, statistically significant positive trends are established only for individual models and seasons (and/or annually), while in the second period 2051-2080, statistically significant trends prevail (except for winter). The highest values by seasons in the second period are 0.98°C/decade in the spring – for CMCC-CM (RCP 4.5), 1.46°C/decade in the summer – for MPI-ESM-MR (RCP 8.5), and 0.88°C/decade in the autumn – for CMCC-CM (RCP 8.5).

The analysis of long-term variations of the projected annual temperatures in the period 1981-2080 shows a significant positive trend, which is better expressed under the scenario RCP 8.5 and comparable with the observed trend in the period 1981-2019.

ACKNOWLEDGMENTS

This study is made with the financial support of the National Program "Young Scientists and Postdoctoral Students" of the Ministry of Education and Science of the Republic of Bulgaria.

Deep gratitude to the organizations and institutions (CMCC, MPI-M, ECMWF, KNMI, Berkeley Earth, Carbon Brief, R Foundation for Statistical Computing), which provide free of charge data and software. Without their innovative data services and tools, this study would not be possible.

The authors would also like to thank Assist. Prof. Dr. Lilia Bocheva for constructive cooperation.

REFERENCES

Bazrkar M.H., Zamani N., Eslamian S., Eslamian A., Dehghan Z. (2015) Urbanization and Climate Change. In: Leal Filho W. (eds) Handbook of Climate Change Adaptation. Springer, Berlin, Heidelberg. https://doi.org/10.1007/978-3-642-38670-1_90

Bellucci, A., Gualdi S., Scoccimarro E., Navarra A. (2008) NAO–ocean circulation interactions in a coupled general circulation model. Climate Dyn., 31, 759-777, doi:10.1007/s00382-008-0408-4.

Blaskova D., Zlatkova L., Lingova S., Modeva J., Sabev L. (1983) Climate and Microclimate of Sofia, Bulgarian Academy of Sciences (in Bulgarian).

Dancheva A., Dimitrova D., Jordanova E., Nikolova G., Kolev M., Kavgadzhiiska S., Mastikova S., Davidkov T., Kateliev S., Filipovich S., Gergova M., Panagonova N., Petkova R., Stoyanova V. (2019) Statistical reference book 2019, NSI010014967, National Statistical Institute

Diaz-Nieto J., Wilby R.L. (2005) A comparison of statistical downscaling and climate change factor methods: impacts on low flows in the River Thames, United Kingdom. Climatic Change 69, 245–268. https://doi.org/10.1007/s10584-005-1157-6

Dimitrova R., Danchovski V., Egova E., Vladimirov E., Sharma A., Gueorguiev O., Ivanov D. (2019) Modeling the Impact of Urbanization on Local Meteorological Conditions in Sofia. Atmosphere 2019, 10, 366.

Friedlingstein P., Andrew R., Rogelj J., Peters G.P., Canadell J.G., Knutti R., Luderer G., Raupach M.R., Schaeffer M., van Vuuren D.P., Le Quéré C. (2014) Persistent growth of CO2 emissions and implications for reaching climate targets. Nature Geosci 7, 709–715. https://doi.org/10.1038/ngeo2248

Giorgetta M.A., Jungclaus J., Reick C.H., Legutke S., Bader J., Böttinger M., Brovkin V., Crueger T., Esch M., Fieg K., Glushak K., Gayler V., Haak H., Hollweg H.D., Ilyina T., Kinne S., Kornblueh L., Matei D., Mauritsen T., Mikolajewicz U., Mueller W., Notz D., Pithan F., Raddatz T., Rast S., Redler R., Roeckner E., Schmidt H., Schnur R., Segschneider J., Six K.D., Stockhause M., Timmreck C., Wegner J., Widmann H., Wieners K.H., Claussen M., Marotzke J., Stevens B. (2013) Climate and carbon cycle changes from 1850 to 2100 in MPI-ESM simulations for the Coupled Model Intercomparison Project phase 5 , Journal of Advances in Modeling Earth Systems, 5 (3), 572-597, doi: 10.1002/jame.20038.

Grimmond, S. (2007), Urbanization and global environmental change: local effects of urban warming. Geographical Journal, 173: 83-88. https://doi.org/10.1111/j.1475-4959.2007.232_3.x

Gualdi S., Scoccimarro E., Navarra A. (2008) Changes in tropical cyclone activity due to global warming: Results from a high-resolution coupled general circulation model. J. Climate, 21, 5204-5228.

Hazeleger W., Severijns C., Semmler T., Ştefănescu S., Yang S., Wang X., Wyser K., Dutra E., Bal-dasano J.M., Bintanja R., Bougeault P., Caballero R., Ekman A.M.L., Christensen J.H., van den Hurk B., Jimenez P., Jones C., Kållberg P., Koenigk T., McGrath R., Miranda P., van Noije T., Palmer T., Parodi J.A., Schmith T., Selten F., Storelvmo T., Sterl A., Tapamo H., Vancop-penolle M., Viterbo P., Willén U. (2010) EC-Earth: a seamless earth-system prediction approach in action. Bulletin of the American Meteorological Society, 91(10), 1357-1364.

Hristov P., Tanev A. (1970) The climate of Sofia, Science and Art State Publishing House (in Bulgarian)

IPCC (2014) Climate Change: Synthesis Report. Contribution of Working Groups I, II and III to the Fifth Assessment Report of the Intergovernmental Panel on Climate Change [Core Writing Team, R.K. Pachauri and L.A. Meyer (eds.)]. IPCC, Geneva, Switzerland, 151 pp.

Ishirkov A. (1903) A few notes on air temperature in Sofia, Journal of Bulgarian literary society, Vol. 63, 114-121 (in Bulgarian)

Kendall M.G., Rank Correlation Methods, 4th ed., Charles Griffin: London, 1975.

Kirov K., Krastanov L. (1938) The Climatological Variations, in "The Climate of Sofia 1887-1937", special edition "50 Years of Meteorological Observations in Sofia", Dragiev&Co, Sofia, 85–95 (in Bulgarian)

Le Quéré C., Andrew R.M., Friedlingstein P., Sitch S., Hauck J., Pongratz J., Pickers P.A., Korsbakken J.I., Peters G.P., Canadell J.G., Arneth A., Arora V.K., Barbero L., Bastos A., Bopp L., Chevallier F., Chini L.P., Ciais P., Doney S.C., Gkritzalis T., Goll D.S., Harris I., Haverd V., Hoffman F.M., Hoppema M., Houghton R.A., Hurtt G., Ilyina T., Jain A.K., Johannessen T., Jones C.D., Kato E., Keeling R.F., Goldewijk K.K., Landschützer P., Lefèvre N., Lienert S., Liu Z., Lombardozzi D., Metzl N., Munro D.R., Nabel J.E.M.S., Nakaok, S., Neill C., Olsen A., Ono T., Patra P., Peregon A., Peters W., Peylin P., Pfeil B., Pierrot D., Poulter B., Rehder G., Resplandy L., Robertson E., Rocher M., Rödenbeck C., Schuster U., Schwinger J., Séférian R., Skjelvan I., Steinhoff T., Sutton A., Tans P.P., Tian H., Tilbrook B., Tubiello F.N., van der Laan-Luijkx I.T., van der Werf G.R., Viovy N., Walker A.P., Wiltshire A.J., Wright R., Zaehle S., Zheng B. (2018) Global Carbon Budget 2018, Earth Syst. Sci. Data, 10, 2141–2194, https://doi.org/10.5194/essd-10-2141-2018.

Madec G., Delecluse P., Imbard M., Levy C. (1998) Opa 8 ocean general circulation model – reference manual. Tech. rep., LODYC/IPSL Note 11.

Marsland S.J., Haak H., Jungclaus J.H., Latif M., Röske F. (2003) The Max- Planck-Institute global ocean/sea ice model with orthogonal curvilinear coordinates. Ocean Modell., 5, 91–127.

Niemelä J., Breuste JH., Guntenspergen G., McIntyre NE., Elmqvist T., James P. (2011) Urban Ecology: Patterns, Processes, and Applications, Oxford University Press, pp. 392

OECD (2010), Cities and Climate Change, OECD Publishing, Paris, https://doi.org/10.1787/9789264091375-en.

OECD (2013), Green Growth in Cities, OECD Green Growth Studies, OECD Publishing, Paris, https://doi.org/10.1787/9789264195325-en.

Oleson K. (2012). Contrasts between Urban and Rural Climate in CCSM4 CMIP5 Climate Change Scenarios, Journal of Climate, 25(5), 1390-1412.

Pohlert T. (2020) trend: Non-Parametric Trend Tests and Change-Point Detection. R package version 1.1.2. https://CRAN.R-project.org/package=trend

R Core Team (2019). R: A language and environment for statistical computing. R Foundation for Statistical Computing, Vienna, Austria. http://www.R-project.org/.

Roeckner E., Bauml G., Bonaventura L., Brokopf R., Esch M., Giorgetta M. A., Hagemann S., Kirchner I., Kornblueh L., Manzini E., Rhodin A., Schlese U., Schulzweida U., Tompkins A.M. (2003) The atmospheric general circulation model ECHAM5 – Part I: Model description, Max-Planck-Institut für Meteorologie, Tech. Rep. 349

Rohde R.A., Hausfather Z. (2020) The Berkeley Earth Land/Ocean Temperature Record, Earth Syst. Sci. Data, 12, 3469–3479, https://doi.org/10.5194/essd-12-3469-2020, 2020.

RStudio Team (2019). RStudio: Integrated Development for R. RStudio, Inc., Boston, MA. http://www.rstudio.com/

Scoccimarro E., Gualdi S., Bellucci A., Sanna A., Giuseppe Fogli P., Manzini E., Vichi M., Oddo P., Navarra A. (2011) Effects of Tropical Cyclones on Ocean Heat Transport in a High-Resolution Coupled General Circulation Model, Journal of Climate, 24(16), 4368-4384.

Seaby L.P., Refsgaard J.C., Sonnenborg T.O., Stisen S., Christensen J.H., Jensen K.H. (2013). Assessment of robustness and significance of climate change signals for an ensemble of distribution-based scaled climate projections. Journal of Hydrology 486(0), 479-493.

Sen P.K. (1968) Estimates of the regression coefficient based on Kendall's tau, Journal of the American Statistical Association 63, 1379–1389.

Shen Z., Shi J., Tan J., Yang H. (2020) The Migration of the Warming Center and Urban Heat Island Effect in Shanghai During Urbanization. Front. Earth Sci. 8:340. doi: 10.3389/feart.2020.00340

Sutton R., Suckling E., Hawkins E. (2015) What does global mean temperature tell us about local climate? Philos. Trans. A Math. Phys. Eng. Sci. 373(2054):20140426. doi: 10.1098/rsta.2014.0426.

Taylor K.E., Stouffer R.J., Meehl G.A. (2012) An Overview of CMIP5 and the Experiment Design, Bulletin of the American Meteorological Society, 93(4), 485-498.

United Nations, Department of Economic and Social Affairs, Population Division (2018) World Urbanization Prospects: The 2018 Revision, Online Edition.

Van Vuuren D.P., Edmonds J., Kainuma M., Riahi K., Thomson A., Hibbard K. (2011) The representative concentration pathways: an overview. Clim. Change. 109:5-31.

Vitanova L.L., Kusaka H. (2018). Study on the urban heat island in Sofia City: Numerical simulations with potential natural vegetation and present land use data. Sustainable Cities and Society, 40, 110-125.

Wang B., Zheng L., Liu D.L., Ji F., Clark A., Yu Q. (2018) Using multi-model ensembles of CMIP5 global climate models to reproduce observed monthly rainfall and temperature with machine learning methods in Australia. Int J Climatol. 38: 4891–4902. https://doi.org/10.1002/joc.5705

Wilby R.L., Charles S.P., Zorita E., Timbal B., Whetton P., Mearns L.O. (2004) Guidelines for use of climate scenarios developed from statistical downscaling methods, Supporting material of the Intergovernmental Panel on Climate Change, available from the DDC of IPCC TGCIA, 27.

World Meteorological Organisation (1996). Climate and Urban development. WMO No. 844, Geneva.

Zorita E., von Storch H. (1999) The analog method as a simple statistical downscaling technique: comparison with more complicated methods. Journal of Climate 12(8), 2474-2489